

## Contrasting geomorphological storm response from two adjacent shorefaces

Joni Backstrom<sup>1</sup>, Derek Jackson<sup>2</sup>, Andrew Cooper<sup>2,3</sup> & Carlos Loureiro<sup>2,3,4</sup>

<sup>1</sup> Independent Marine Consultant, Wilmington, NC 28403, USA

<sup>2</sup> School of Environmental Sciences, Ulster University, Coleraine, BT52 1SA, UK

<sup>3</sup> School of Agriculture, Earth and Environmental Sciences, University of KwaZulu-Natal, Private Bag X54001, Durban, South Africa

<sup>4</sup> Centro de Investigação Marinha e Ambiental, Universidade do Algarve, Campus de Gambelas, 8005-139 Faro, Portugal

**Keywords:** shoreface, storms, sediment transport, numerical modeling, North Atlantic

This article has been accepted for publication and undergone full peer review but has not been through the copyediting, typesetting, pagination and proofreading process which may lead to differences between this version and the Version of Record. Please cite this article as doi: 10.1002/esp.3788

## Abstract

Shorefaces play a critical role in cross-shore sediment transport between the beach and inner shelf, particularly during storm conditions. A comparison and examination of storm-driven sedimentary changes on two adjacent shorefaces in Northern Ireland, located only five kilometres apart, revealed significantly different geomorphological responses. The steeper shoreface at West Strand responded with extensive sediment deposition across almost the entire shoreface, in contrast to the more dissipative and quasi-linear shoreface at Portstewart, which mostly showed nearshore bar changes. Results from the two sites, which have similar wave/wind characteristics and seabed sediments, suggest that: i) cross-shore morphology, ii) immediately previous (antecedent) shoreface morphodynamic behaviour and iii) the presence, or lack of, offshore sand appear to be the primary controls on storm-driven sedimentary changes attributed to the high-energy event.

## Introduction

The shoreface plays a critical role in diabathic (cross-shore) sediment transport and distribution between the inner shelf and beach (Niedoroda and Swift, 1981; Cowell *et al.*, 1999; Anthony *et al.*, 2006; Hequette *et al.*, 2008; Anthony, 2013). This friction-dominated coastal environment plays a key role in storm response (Wright *et al.*, 1986), sediment exchange (Stive *et al.*, 1991) and response to long-term sea level changes (Roy *et al.*, 1994; Cowell *et al.*, 1995; Stive, 2004). The shoreface is a poorly understood transition zone that is continuously changing form in response to dynamic conditions (Niedoroda *et al.*, 1985; Wright *et al.*, 1991; Backstrom *et al.*, 2007, 2009b). Although scientific knowledge of shoreface dynamics has improved significantly over the last few decades, it is not possible to empirically and/or numerically predict process-response mechanisms across this complex environment (Thieler *et al.*, 2000; Cooper and Pilkey, 2004).

Although there is an abundance of scientific literature on event-scale beach and surf zone dynamics (Wright and Short, 1984; Aagard and Masselink, 1999; Short and Jackson, 2013), much less is known about the morphological response of the shoreface to storm events. It is generally agreed that short-term high-magnitude events often cause much larger coastal change than long intervening periods of fair weather (Carter, 1988). Storm events typically result in beach erosion and offshore deposition of sand in the form of bars, which are subsequently reworked landward under fair-weather conditions (Komar, 1976; Lee *et al.*, 1998). The cross-shore sediment exchange at the coast, however, extends seaward of the surf zone (Smith *et al.*, 2010). Near-bottom wave orbital velocities associated with storm events entrain sand over the entire shoreface; the sand is subsequently distributed by currents along and across the shoreface and inner shelf (Niedoroda *et al.*, 1984). The magnitude of change is typically a depth, energy and time dependent relationship; i.e. shallower depths, larger storms

and longer time periods result in greater morphological change (Cowell *et al.*, 1999; Hinton and Nicholls, 2007).

In this paper, we document the morphological storm response of two geomorphologically different but geographically adjacent (5 km apart) shorefaces and relate this to wave hydrodynamics.

## **Study Areas**

### **North coast of Northern Ireland**

The study areas are located along the north coast of Northern Ireland, a high-energy, headland embayment coastline (Fig. 1) which is periodically exposed to storms and large swells from the North Atlantic. The coast is punctuated by basaltic headlands and cliffs, while sandy beaches and large coastal dunes are present in coastline re-entrants (Jackson *et al.*, 2005).

Tidal regime at both study sites is microtidal and semi-diurnal, with a mean tidal range of 1.3 m (British Oceanographic Data Center (BODC) tide gauge, Portrush). Mean spring tidal range is approximately 2 metres. Mean significant wave heights ( $H_s$ ), based on a calculated wave-grid location 10 km offshore in 35 m water depth, are 1.35 m with an 8.5 s period (UK Met Office, 2000-2005). However,  $H_s$  in winter swells can exceed 5 m with up to 18 s wave periods (Carter, 1991). As SW swell waves approach the northwest coast of Ireland, they are refracted southwards towards the north-facing beaches of Northern Ireland. Wind is predominantly from the west/southwest (cross-offshore), and gale force winds are common, particularly in the winter. Surficial sediments at both sites consist of fine-grained, well-sorted quartz sand with a mean diameter of 0.17 mm (Backstrom *et al.*, 2007). The thickness of this upper sand unit ranges from <1 m to 5 m and is underlain by bedrock and/or glacial sediments (Cooper *et al.*, 2002).

Multibeam bathymetric surveys conducted by the Joint Irish Bathymetric Survey (JIBS) off the north coast of Northern Ireland in 2007 have revealed the presence of extensive and widespread mobile bedforms and other large sand bodies located in >20 m depth, particularly offshore of West Strand (see Plets *et al.*, 2012).

### **Portstewart Strand**

Portstewart Strand is a 3 km long dissipative beach backed by an extensive, up to 25 m high, vegetated dune system. The beach is located between the Bann river-mouth/jetties to the west and a basaltic headland in the east (Fig. 1). Subtidal sediment thickness ranges from approximately 5 m nearshore, to less than 1 m thickness in the lower shoreface at approximately 20 m depths, where exposed bedrock with a veneer of surface sediment is present (Cooper *et al.*, 2002).

### **West Strand**

The second site is West Strand, Portrush, located approximately 5 km east of Portstewart (Fig. 1). This is an 800 m long embayment beach, constrained on both sides by basaltic headlands and rocky shorelines. The beach has been modified considerably by engineering works since the 1800's, including a small harbour built in 1825 and a recurved seawall/promenade (1960's) that extends along the back of the beach. The construction of the seawall/promenade resulted in the final removal of an extensive dune system which had previously backed the beach (Carter, 1991). Peat is often exposed on the southwest part of the sub-aerial beach (Westley *et al.*, 2014) following storm conditions, confirming the presence of only a thin veneer of modern surface sediments along the beach and intertidal area.

**Insert Figure 1.**

## **Methods**

A series of shore-normal bathymetric survey lines, ranging from 1 – 20 m depths and 75-150 m spacing (Fig. 1), were undertaken at both locations with a MIDAS SURVEYOR hydrographic survey system. Depth (210 kHz, accuracy 0.10 m) and DGPS position (WGS 1984, accuracy 1-3 m) were collected every second, providing x,y,z data at 2-3 m intervals. The data were filtered for anomalies, and tide corrected to mean sea-level using the British Oceanographic Data Centre (BODC) tide gauge located in Portrush Harbour. All position data were further converted into (metric) Irish Grid coordinate system to improve geographic mapping capabilities.

Pre- and post-storm surveys were conducted 11 days before and 4 days after a storm event on June 22<sup>nd</sup>, 2006. Pre- and post-storm surveys occupied the same survey lines. The tide-corrected x,y,z data were interpolated using triangulation (TIN) and converted into a grid with 10 x 10 m cell dimensions. In order to analyse the changes between subsequent surveys, the pre-storm gridded data was subtracted from the post-storm grid in Arcview. This analysis method provided a gridded dataset map, showing areas of erosion, deposition and no change between surveys.

Hindcast offshore wave data for Northern Ireland were provided by the Met Office UK Waters Wave Model (Golding, 1983; Bradbury *et al.*, 2004) for a grid point 10 km offshore of the study sites, located in 35 m water depth (55.28°N; 6.75°W). Data included significant wave height ( $H_s$ ), wave period ( $T_z$ ) and wave direction ( $\theta$ ) at 3-hour intervals, which were used to evaluate offshore wave conditions and as input for the nearshore propagation SWAN wave model (Booij *et al.*, 1999; Ris *et al.*, 1999). SWAN was run at 3-hour intervals from the 20th to the 24th of June with the parametric hindcast wave data uniformly applied to the

offshore boundary, considering a JONSWAP spectral shape to represent the wave field, and variable water levels (obtained from the hourly records from Portrush Harbour tide gauge). SWAN was run in third-generation mode, and accounted for default linear wave growth and whitecapping dissipation, nonlinear triad wave-wave interactions, bottom friction dissipation using a variable JONSWAP expression following Hasselmann *et al.* (1973), breaking dissipation according to the default bore-based model of Battjes and Janssen (1978) and depth-induced wave breaking in shallow water imposed by a scaled breaker index according to the  $\beta$ -kd model for surf-breaking (Salmon and Holthuijsen, 2011). The wave frequency and directional space were discretized in 30 logarithmic-distributed bins from 0.03 Hz to 1.00 Hz and 36 regular-distributed bins, respectively. The modelling domain extended  $\sim$ 33 km alongshore, centered on the study sites, and 12 km offshore from the shoreline, to water depths between 30 and 130 m below mean sea level. A regular grid with 5 m resolution was used to represent the bottom levels within the modelling domain, obtained from the high-resolution multibeam bathymetry data collected in December 2007 by the Joint Irish Bathymetric Survey.

SWAN outputs were computed for the entire modelling domain and variables extracted for analysis included significant wave height ( $H_s$ ), wave length ( $L$ ), water depth ( $h$ ), the root-mean-square of the maximum wave orbital velocity near the bottom ( $U_{orb}$ ), and energy dissipation due to bottom friction ( $ED_{bot}$ ). The latter is computed from the action balance equation that includes a term for energy dissipation (detailed in Booij *et al.*, 1999; Ris *et al.*, 1999). This term considers a contribution of dissipation due to bottom friction, as this is the primary mechanism of energy dissipation in shallow water prior to breaking (Ris *et al.*, 1999). For operational reasons the bottom friction term in SWAN considers empirical approximations based on a bottom friction coefficient and the wave-induced motion of the water particles within the turbulent boundary layer at the bottom. These are obtained from the

JONSWAP model and from the root-mean-square orbital bottom velocity computed using linear wave theory (Holthuijsen, 2007).

## **Results**

### **Pre-storm shoreface morphology**

A comparison of cross-shore bathymetric profiles for both sites is presented in Figure 2 (selected from centrally located profile lines). The Portstewart profile is characterised by a nearshore bar and trough located landward of 5 m depth. Seaward of 5 m depth, the profile becomes quasi-linear and relatively gentle ( $0.74^\circ$ ) to the 20 m depth contour, approximately 1600 m offshore. Beyond 20 m depth, the profile becomes sub-horizontal and more irregular in shape, primarily due to exposure of underlying gravels and bedrock.

The shoreface profile at West Strand is concave-up, typical of many documented shorefaces (Dean, 1977; Wright *et al.*, 1991). The nearshore profile consists of a series of small ( $< 1$  m high) bars and troughs, out to approximately 4 m depth. Seaward of 4 m depth the profile steepens, reaching 15 m depth approximately 700 m offshore ( $1.22^\circ$ ). At 18 m depth, or approximately 1200 m from the coast, the seabed profile becomes sub-horizontal.

**Insert Figure 2.**

### **Storm Characteristics**

Offshore wave heights, wave period, wave direction and tidal data from the pre- to post-storm surveys (June 11<sup>th</sup> - 27<sup>th</sup>, 2006) are presented in Figure 3. Prior to the onset of the storm, offshore significant wave heights ranged from 0.5 to 1.5 m, mean wave periods were in the range of 8.5 to 4 s from a northwesterly to northerly direction. The storm lasted three days, from June 20<sup>th</sup> to 23<sup>rd</sup>. During the peak of the storm, between June 21<sup>st</sup> and 22<sup>nd</sup>, offshore



wave heights reached a maximum of 3.7 m, mean wave periods increased consistently up to 9 s during the first day of the storm and then decreased to values around 6 s by the end of the storm period. Mean wave direction gradually shifted from the southwest prior to the onset of the storm, to a northwesterly direction during its peak, reflecting the regular direction of storm events that reach the coast of Northern Ireland. Following the storm, and up until the post-storm survey on June 26th, offshore wave heights and periods dropped quickly to less than 1 m and less than 6 s, respectively. Wind direction remained constant from a northerly quadrant. Tide data (Fig. 3) reveals that the peak of the storm coincided with a 1.1 m high tide at 03:00 on June 22nd.

**Insert Figure 3.**

### **Post-storm Analysis**

The morphological response of both study sites was obtained by comparing the pre- and post-storm bathymetric profiles and GIS-generated shoreface grids. A plan view of the spatial arrangement of areas of erosion (dark gray to black), deposition (light gray) and no change (white) provided key information about storm-driven shoreface morphodynamics and sedimentary processes for both locations.

#### Portstewart

The storm-associated morphologic response of the Portstewart shoreface is shown in Figure 4. A comparison of pre- and post-storm grids reveals that the storm response at this location was not significant, with only highly localised erosion in 3 – 4 m depths, where nearshore bars are present (Backstrom *et al.*, 2009a). No measurable change was observed from 5 to 20 m depth. Minor morphological change was recorded seaward of 20 m, with localised and

patchy areas of accretion and erosion. The storm resulted in a net volume gain of  $\sim 16,340 \text{ m}^3$  of sediment spread across the shoreface study area.

**Insert Figure 4.**

#### West Strand, Portrush

Storm-associated morphological changes involved significant sediment deposition across almost the entire nearshore and shoreface at West Strand (Fig. 5). Deposition was most pronounced adjacent to the harbour entrance, with up to 1.6 m of accretion in 5 m water depth. Sediment deposition across the rest of the shoreface was typically about 0.5 m. A narrow, shore-parallel area of no change was observed in 2 - 3 m water depths. The only areas of erosion were three very minor zones ( $< 500 \text{ m}^2$  each) at the very southwest margin of the study area, between 1 and 4 m water depths. Results of post-storm analysis revealed a net gain of  $596,337 \text{ m}^3$ , equivalent to approximately 49 cm of deposition across the study area.

**Insert Figure 5.**

#### **Numerical Modelling**

Modelled nearshore wave characteristics during the storm demonstrate a progressive onshore reduction in wave height, but with noticeable variations between the two study sites (Fig. 6). At the peak of the storm (05:00 on the 21<sup>st</sup> to 10:00 on the 22<sup>nd</sup>), wave heights at 20 m depth were marginally higher at West Strand (Fig. 6h) compared to Portstewart (Fig. 6d). At 15 m and 10 m water depth the wave heights were practically unchanged at Portstewart, with  $H_s$  peaking at  $\sim 3\text{m}$  (Fig. 6b and 6c), while at West Strand a marked reduction occurs, with maximum  $H_s$  not exceeding 2.5 m in 10 m water depth (Fig. 6f). Closer to shore, the

differences in wave conditions between the two sites increase. At 5 m water depth  $H_s$  at Portstewart was 0.5 m higher than at West Strand (Fig. 6a and 6e).

**Insert Figure 6.**

From the cross-shore profile of modelled energy dissipation due to bottom friction for the maximum  $H_s$  during the storm, it is possible to identify the depth-dependent energy dissipation, with the general trend of increasing dissipation with decreasing depth (Fig. 7). Portstewart Strand presents a consistently increasing energy dissipation profile, with three distinct peaks with decreasing  $ED_{\text{bot}}$  (Energy Dissipation at the seabed) at offshore distances of 620 m (-7.5 m), 350 m (-4.9 m) and 175 m (-2.5 m) (Fig. 7a). For West Strand,  $ED_{\text{bot}}$  increase is very subtle up to a distance of 750 m from the shoreline (Fig. 7b), becoming more pronounced in a shoreward direction and peaking at a distance of 210 m from the shoreline, at approximately 4.5 m depth.

**Insert Figure 7.**

Considering that near-bed sediment movement depends on the bottom orbital velocity amplitude (Soulsby, 1997), and this can be approximated using  $U_{\text{bot}}$  (e.g. Oberle *et al.*, 2014), modelled  $U_{\text{bot}}$  values are presented as an indicator for the potential of near-bed sediment movement (given the homogeneity in grain size within the study areas, as presented in Backstrom *et al.* (2007) and Plets *et al.* (2012)). The cross-shore profiles of  $U_{\text{bot}}$  for each site (across the centre of the study areas) during the maximum  $H_s$ , (Fig. 8) are identical to  $ED_{\text{bot}}$  profiles, presenting similar patterns and near-bottom velocity peaks corresponding exactly to peaks in energy dissipation.  $U_{\text{bot}}$  velocities are consistently above  $0.5 \text{ ms}^{-1}$  in West Strand

(Fig. 8b), while for Portstewart Strand sections deeper than ~18 m  $U_{\text{bot}}$  is between 0.4 and 0.5  $\text{ms}^{-1}$  (Fig. 8a). Inversely, closer to shore and particularly at sections shallower than 12 m,  $U_{\text{bot}}$  velocities are higher in Portstewart Strand, consistently above 0.8  $\text{ms}^{-1}$ , while at West Strand  $U_{\text{bot}}$  barely reaches 0.8  $\text{ms}^{-1}$  for similar depths. The cross-shore profiles of near-bed orbital velocities (Fig. 8) demonstrate, logically, the increased potential for sediment movement across an extended surfzone during high-energy events, but demonstrate also that under high waves, conditions for sediment movement are widespread across the shoreface.

Modelling results for the storm conditions indicate distinct differences in wave transformation across the shoreface of Portstewart and West Strand, despite the proximity between the two sites. Wave attenuation is higher at West Strand, as evidenced by significantly lower wave heights at 5 m and 10 m water depths (Fig. 6), and the profiles of energy dissipation due to bottom friction are also distinct, reflecting the differences in shoreface profile between the two sites (Fig. 7). Energy dissipation, seaward of the surf zone, is mainly confined to the near-bed boundary layer (Fredsoe and Deigaard, 1992), and occurs due to complex mechanisms in the relatively thin turbulent boundary layer at the bottom created by wave-induced motion of water particles (Holthuijsen, 2007). Despite such complexity, sediment transport seaward of the surf zone is mainly driven by the magnitude and asymmetry of the orbital wave-velocities at the bottom (Fredsoe and Deigaard, 1992). As  $U_{\text{bot}}$  velocities greater than 0.2  $\text{ms}^{-1}$  are able to mobilise fine sand during moderate to high-energy wave conditions in a storm-dominated shelf (Oberle *et al.*, 2014), and that generalized wave-induced fine sand movement occurs once orbital velocities exceed a threshold of 0.25  $\text{ms}^{-1}$  (Soulsby, 1997),  $U_{\text{bot}}$  values above 0.4  $\text{ms}^{-1}$  for the peak of the storm for the entire shoreface of both Portstewart and West Strand (Fig. 8) are a clear indication of potential for sediment transport. The presence of coarse to fine sand in the inner shelf adjacent (and beyond) the study area and fronting the West Strand shoreface (Plets *et al.*, 2012), combined

with large-scale sand-waves indicative of sediment transport (Fig. 9), while at Portstewart the inner shelf is characterised by the presence of rock outcrops (Plets *et al.*, 2012; Fig. 9), it is reasonable to assume that despite suitable wave-induced conditions for near-bottom sediment transport in both shorefaces, the differences in storm-induced morphological change reflect mostly differences in sediment availability in the inner shelf adjacent to each site.

**Insert Figure 8.**

## **Discussion**

It is apparent from the pre- and post-storm bathymetric comparisons that the two shorefaces exhibited different geomorphological responses to the storm event. While the low gradient dissipative Portstewart shoreface exhibited minor nearshore bar changes, the steeper concave shoreface at West Strand responded *via* significant shoreface-wide accretion. Since both locations have similar surficial sediments and the storm forcing was identical, the morphological changes observed must be attributed to: i) differences in shore-normal morphology, and ii) availability or paucity of offshore sand for mobilisation.

Shoreface gradients play a key role in how much incoming wave energy is expended across the shoreface and nearshore (Battjes and Janssen, 1978). Nearshore equilibrium models also tend to assume a balance between asymmetrical orbital velocities and slope (Bowen, 1980; Bailard and Inman, 1981). Wave modelling of morphological response to relative sea-level rise in the Netherlands suggest that shoreface slopes control wave energy dissipation, and consequently, shoreface profile adjustment and surficial sediment properties (Cowell, 2000a). Numerical modelling investigations by Roy *et al.* (1994) demonstrated that steep shorefaces (with gradients  $> 0.8^\circ$ ) are more likely to have offshore-directed sediment transport than dissipative and shallow shorefaces, which have a tendency towards nearshore accretion.

The shoreface profiles for both study sites are markedly different; Portstewart is relatively linear and dissipative compared to West Strand, which has a steep upper shoreface and is more reflective (refer to Fig. 2). Wave theory therefore suggests that less energy will reach the nearshore and upper shoreface at Portstewart, since frictional interaction with the seabed should be greater along the linear, dissipative shoreface compared to the steeper, concave profile at West Strand.

Field studies have also shown that coastal/shoreface configuration plays a dominant role in sediment transport during storm conditions. Hequette *et al.* (2001) demonstrated that a steep nearshore zone backed by coastal bluffs favoured strong offshore-directed shoreface sediment transport under storm conditions compared to adjacent barrier-island coasts. An examination of storm-driven sedimentary changes off a low-energy delta in southern Spain also revealed contrasting nearshore and shoreface responses, depending on shoreline orientation and coastal gradients (Backstrom *et al.*, 2008). Seismic reflection studies have also shown that steep shorefaces tend to have thicker sand deposits offshore than lower angled shorefaces, suggesting seaward-directed sediment transport, particularly during storms (Field and Roy, 1984).

Offshore sediment transport and shoreface deposition, accompanied by a long-term trend of beach erosion has been documented off the Delaware coast (Csanady, 1977) and Tiana Beach, Long Island, New York (Niedoroda and Swift, 1981). Results from these locations suggest that storms terminate the shoreface steepening process (landward sediment transport from the shoreface during fair-weather conditions), through shoreface sediment accumulation and landward translation of the profile.

However, there are also many studies, over a range of temporal scales, which show landward sediment transport directed from the inner shelf and lower shoreface towards the upper shoreface, surf-zone and beach. Seismic studies, coupled with radiometric dating in Australia,

have confirmed significant strandplain (prograded beach) development along a headland-embayment coast, attributed to the last ~ 6,000 years as sea levels have risen (Cowell *et al.*, 2000b). Long term bathymetry investigations, extending over 70 years, off the Pacific coast of the USA (Kaminsky *et al.*, 1999) and the coast of The Netherlands (Stive and deVriend, 1995) also confirm inner shelf erosion with resultant upper shoreface deposition, suggesting landward sediment transport from deeper water. Similar long-term studies have also been documented off the Danish coast, confirming the lower shoreface acts as a source of sediment, which feeds the surf zone, beach and dunes (Aagaard *et al.*, 2004).

Short-term sedimentary changes associated with a northeaster off the concave nearshore/shoreface at Duck, North Carolina, showed rapid bed accretion after a period of erosion, for a total bed elevation change of +15 cm (Wright *et al.*, 1986). Shoreface accretion was attributed to the offshore or alongshore movement of sand bodies in deeper water associated with nearbed currents. Schwab *et al.* (2000, 2013) have suggested significant inner shelf sediment supply to the shoreface off the western coast of Fire Island, NY, particularly during storm events. These storm events may actually contribute to long-term beach accretion, contrary to expectations. Therefore it is reasonable to suggest onshore-directed sediment transport occurred from the inner shelf towards the shoreface at West Strand, which may have taken place either during the storm or during the latter stages of it. The numerical modelling results presented earlier also confirm that hydrodynamic energy was more than sufficient to mobilise and transport the fine sands across the entire shoreface.

The origin of the significant volume of sand deposited on the West Strand shoreface (50 cm m<sup>-2</sup>) was initially problematic. Since the embayment beach is situated between two rocky headlands, it is unlikely that the sand came from adjoining shorefaces. The volume of material eroded from the sub-aerial beach during the event may have contributed to some of the accretion, but is still not enough to explain the 596,337 m<sup>3</sup> of net shoreface deposition

(e.g. a conservative 0.5 m erosion of the 57,000 m<sup>2</sup> beach would only yield 28,500 m<sup>3</sup> of sand). Therefore, the source of the deposited sand must have been from offshore, seaward of the survey area. There are two pieces of evidence to suggest that the offshore region is the origin of the significant sediment accumulation at West Strand.

Periodic, quasi-monthly, bathymetric surveys off West Strand over a two-year period (between 2005 and 2007) revealed a complex pattern of shoreface-wide erosion and deposition, which was not always directly linked to wave forcing (Backstrom *et al.*, 2009a). The antecedent shoreface morphology played a key role in how the shoreface responded to wave forcing. For example, if there was significant shoreface erosion in a previous survey, results often showed subsequent shoreface accretion, and vice versa. A survey conducted before this particular high-energy event (between April and June 2006), showed significant shoreface erosion, with a net loss of 306,577 m<sup>3</sup>, which is comparable to the volume of sediment introduced during this post-storm survey. It is therefore reasonable to believe that the sand, which had been eroded from the survey area previously and deposited seaward of the study area, was available for subsequent mobilisation and deposition back onto the shoreface during the storm.

Prior to 2007, there were no regional or high-resolution geophysical offshore datasets for this part of the Northern Irish coast, apart from some widely-spaced seismic lines collected by Cooper *et al.*, (2002). Geophysical data collected by the JIBS in 2007, including multibeam bathymetry data, covering large swathes of the northern Irish offshore region, has revealed the presence of large and significant sand bodies in 30-50 m depths (Fig. 9), especially offshore of West Strand. These large mobile bedforms are not present offshore of Portstewart. The discovery of these large offshore deposits, particularly off West Strand, helps explain the likely source of sand which was available for re-entrainment and deposition during the storm.



In contrast, the absence of offshore sand off Portstewart (confirmed with the presence of subcropping bedrock in 20 m depths and JIBS/GSI data) constrained the availability of sediment for shoreface sedimentation. Instead, most of the observed changes were spatially confined and occurred close to shore in the form of nearshore bar changes, rather than extensive accretion or erosion.

### **Insert Figure 9.**

The nearshore pattern of changes at Portstewart is in agreement with expected beach and shoreface morphodynamics for dissipative beaches (Wright and Short 1984) and in line with the predicted behaviour after two years of survey observations (Backstrom *et al.*, 2009b). It is suggested that the dissipative nature and the availability of nearshore sand in the form of large coastal dunes (which directly back the beach) allows Portstewart to be in an equilibrium stage with oceanographic forcing, even during storm events. In contrast, shoreface wide deposition observed at West Strand is attributed to shoreward sediment transport from the inner shelf, where the source sediment comprises large sand bodies located in deeper water.

### **Conclusions**

The morphological response of two adjacent shorefaces to high-energy storm forcing has shown important differences in sedimentary morphodynamics. The results strongly suggest that antecedent shoreface morphology, gradients and the availability of either terrestrial sand sources in the form of dunes, or inner shelf sand sources in the form of large bedforms, exerts a major control on sediment transport mechanisms and dynamics during storm events.

With large uncertainty regarding changes in storminess, but significant relative sea level rise due to climate change, combined with a growing coastal population, it is imperative that an

improved understanding of storm morphodynamics, from the beach to the inner shelf, takes greater precedence. Although a substantial amount of scientific literature exists on beach and surf zone dynamics, our understanding of shoreface behaviour is still limited. Understanding the morphological response of shorefaces with different morphologies and sedimentary environments to storm events is critical, given that the shoreface, and inner shelf, ultimately play a crucial role in controlling coastal dynamics. Acting as a sediment store and an effective energy buffer during storms, it represents an important interface zone between the open ocean and the coastal zone.

## **Acknowledgments**

This research was funded by the Vice Chancellors Research Scholarship from Ulster University. The authors would especially like to thank all the students and staff who assisted with offshore surveys. CL was supported by Fundação para a Ciência e Tecnologia (grant reference SFRH/BPD/85335/2912).

This research would not have been complete without the JIBS data made available by the Maritime and Coast Guard Agency (UK), the Marine Institute of Ireland, the Northern Ireland Environment Agency (NIEA) and the Geological Surveys of Ireland (GSI) and Northern Ireland (GSNI). The authors would also like to thank the UK Met Office for kindly providing hindcast wave data.

## References

- Aagaard, T., and Masselink, G., 1999. The Surf Zone. In: Short, A.D. (ed.) *Handbook of Beach and Shoreface Morphodynamics*. John Wiley and Sons Ltd., Chichester, pp. 72-118.
- Aagaard, T., Davidson-Arnott, R., Greenwood, B., and Nielsen, J., 2004. Sediment supply from shoreface to dunes: linking sediment transport measurements and long-term morphological evolution. *Geomorphology* 60, 205-224.
- Anthony, E.J., Vanhee, S. and Ruz, M-H. 2006. Short-term beach–dune sand budgets on the North Sea coast of France: Sand supply from shoreface to dunes, and the role of wind and fetch. *Geomorphology*, 81, 316-329.
- Anthony, E.J. 2013 Storms, shoreface morphodynamics, sand supply, and the accretion and erosion of coastal dune barriers in the southern North Sea. *Geomorphology*, 199, 8-21.
- Backstrom, J.T., Jackson, D.W.T., and Cooper, J.A.G., 2007. Shoreface dynamics of two high-energy beaches in Northern Ireland. *Journal of Coastal Research*, SI 50, 594-598.
- Backstrom, J.T., Jackson, D.W.T., Cooper, J.A.G. and Malvarez, G.C., 2008. Storm-driven shoreface morphodynamics on a low-wave energy delta: the role of nearshore topography and shoreline orientation. *Journal of Coastal Research*, 24, 1379-1387.
- Backstrom, J.T., Jackson, D.W.T., and Cooper, J.A.G., 2009a. Shoreface morphodynamics of a high-energy, steep and geologically constrained shoreline segment in Northern Ireland. *Marine Geology*, 257, 94-106.
- Backstrom, J.T., Jackson, D.W.T., and Cooper, J.A.G., 2009b. Contemporary morphodynamics of a high-energy headland-embayment shoreface. *Continental Shelf Research*, 29, 1361-1372.
- Bailard, J.A., and Inman, D.L., 1981. An energetics bedload model for a plane sloping beach: Local transport. *Journal of Geophysical Research*, 86, 10938-10954.
- Battjes J.A., Janssen J.P.F.M., 1978. Energy loss and set-up due to breaking of random waves. Proceedings of the 16th International Conference on Coastal Engineering. ASCE, pp. 569–587.
- Booij N., Ris R.C., Holthuijsen L.H., 1999. A third-generation wave model for coastal regions - 1. Model description and validation. *Journal of Geophysical Research*, 104, 7649–7666.

- Bowen, 1980. Simple models of nearshore sedimentation; beach profiles and longshore bars. In: McCann, S.B. (ed.) *The coastline of Canada*. Geological Society of Canada, Paper 80-10, 1-11.
- Bradbury A.P., Mason T.E., Holt M.W., 2004. Comparison of the performance of the Met Office UK-Waters wave model with a network of shallow water moored buoy data. Proceedings of the 8th International Workshop on Wave Hindcasting and Forecasting. WMO Technical Document No. 1319. G1-15p.
- Carter, R.W.G., 1988. *Coastal Environments*. Academic Press, London.
- Carter, R.W.G., 1991. *Shifting sands: A Study of the Coast of Northern Ireland from Magilligan to Larne*. Department of the Environment, Belfast.
- Cooper, J.A.G., Kelley, J.T., Belknap, D.F., Quinn, R., and McKenna, J., 2002. Inner shelf seismic stratigraphy off the north coast of Northern Ireland: new data on the depth of the Holocene lowstand. *Marine Geology*, 186, 369-387.
- Cooper, J.A.G., and Pilkey, O. H., 2004. Alternatives to the mathematical modelling of beaches. *Journal of Coastal Research*, 20, 641-644.
- Cowell, P.J., Roy, P.S., and Jones, R.A., 1995. Simulation of large-scale coastal change using a morphological behaviour model. *Marine Geology*, 126, 45-61.
- Cowell, P.J., Hanslow D.J., and Meleo, J., 1999. The Shoreface. In: Short, A.D. (ed.) *Handbook of Beach and Shoreface Morphodynamics*. John Wiley and Sons Ltd., Chichester, 39-71.
- Cowell, P.J., 2000a. Modelling the decrease in wave height over the shoreface due to slope-induced changes in bottom friction. In: Cleveringa, J., (ed.) *Reconstruction and Modelling of Holocene Coastal Evolution of the Western Netherlands*. University of Utrecht, Netherlands, 133-144.
- Cowell, P.J., Stive, J.F.M., Roy, P.S., Kaminsky, G.M., Buijsman, M.C., Thom, B.G., and Wright, L.D., 2000b. Shoreface sand supply to beaches. *Coastal Engineering*, 2000: pp. 2495-2508.
- Csanady, G.T., 1977. The coastal jet conceptual model in the dynamics of shallow seas. In: Goldberg, E.D., McCave, I.N., O'Brien, J.J., and Steele, J.H., (eds.) *The Sea*, 6, 117-144.
- Dean, R.G., 1977. Equilibrium beach profiles: U.S. Atlantic and Gulf Coasts. *Ocean Engineering Technical Report, no. 12*. University of Delaware, Newark.

- Field, M.E., and Roy, P.S., 1984. Offshore transport and sand body formation: evidence from a steep, high energy shoreface, Southeastern Australia. *Journal of Sedimentary Petrology*, 54, 1292-1302.
- Fredsoe J., Deigaard R., 1992. Mechanics of coastal sediment transport. *World Scientific Publishing*, Singapore. 369 p.
- Golding B., 1983. A wave prediction system for real-time sea-state forecasting. *Quarterly Journal Royal Meteorological Society*, 109, 393-416.
- Hasselmann K., Barnett T.P., Bows E., Carlson H., Cartwright D.E., Enke K., Ewing J.A., Gienapp H., Hasselmann D.E., Kruseman P., Meerburg A., Müller P., Olbers D.J., Richter K., Sell W., Walden H., 1973. Measurements of wind-wave growth and swell decay during the Joint North Sea Wave Project (JONSWAP). *Ergänzungsheft zur Deutschen Hydrographischen Zeitschrift*, A8 (12), 1-95.
- Hequette, A., Desrosiers, M., Hill, P.R., and Forbes, D.L., 2001. The influence of coastal morphology on shoreface sediment transport under storm-combined flows, Canadian Beaufort Sea. *Journal of Coastal Research*, 17, 507-516.
- Hequette, A., Hemdane, Y. and Anthony, E.J., 2008. Sediment transport under wave and current combined flows on a tide-dominated shoreface, northern coast of France. *Marine Geology*, 249, (3-4), 226-242.
- Holthuijsen, L.H., 2007. *Waves in Oceanic and Coastal Waters*. Cambridge University Press, Cambridge.
- Hinton, C.L., and Nicholls, R.J., 2007. Shoreface morphodynamics along the Holland Coast. In: Balson, P.S., and Collins, M.B. (eds) *Coastal and Shelf Sediment Transport*. Geological Society of London, Special Publications, 274, 93-101.
- Jackson, D.W.T., Cooper, J.A.G., and Del Rio, L., 2005. Geological control of beach morphodynamic state. *Marine Geology*, 216, 297-314.
- Kaminsky, G.M., Buijsman, M., Gelfenbaum, G., Ruggiero, P., Jol, H.M., Gibbs, A.E., and Peterson, C.D., 1999. Synthesizing geological observations and process-response data for modeling coastal change at management scale. Coastal Sediments '99, ASCE, 1660-1675.
- Komar, P.D., 1976. *Beach Processes and Sedimentation*. Prentice Hall, Inc., New Jersey.
- Lee, G., Nicholls, R.J., and Birkemeier, W.A., 1998. Storm-driven variability of the beach-nearshore profile at Duck, North Carolina, USA, 1981-1991. *Marine Geology*, 148, 163-177.

- Niedoroda, A.W., and Swift, D.J.P., 1981. Maintenance of the shoreface by wave orbital currents and mean flow: observations from the Long Island Coast. *Geophysical Research Letters*, 8, 337-348.
- Niedoroda, A.W., Swift, D.J.P., Hopkins, T.S., and Ma, C.M., 1984. Shoreface morphodynamics of wave-dominated coasts. *Marine Geology*, 60, 331-354.
- Niedoroda, A.W., Swift, D.J.P., and Hopkins, T.S., 1985. The shoreface. In: Davis, R.A. (ed.) *Coastal Sedimentary Environments*, Springer, New York, 533–624.
- Oberle, F.K.J., Storlazzi, C.D., Hanebuth, T.J.J., 2014. Wave-driven sediment mobilization on a storm-controlled continental shelf (Northwest Iberia). *Journal of Marine Systems*, 139, 362-372.
- Plets, R., Clements, A., Quinn, R., Strong, J., 2012. Marine substratum map of the Causeway Coast, Northern Ireland. *Journal of Maps*, 8, 1-13.
- Ris, R.C., Holthuijsen, L.H., Booij, N., 1999. A third-generation wave model for coastal regions - 2. Verification. *Journal of Geophysical Research*, 104 (C4), 7667–7681.
- Roy, P.S., Cowell, P.J., Ferland, M.A., and Thom, B.G., 1994. Wave dominated coasts. In: Carter, R.W.G. and Woodroffe, C.D. (eds.), *Coastal Evolution: Late Quaternary Shoreline Morphodynamics*. Cambridge University Press, Cambridge, 33-86.
- Salmon, J., Holthuijsen, L., 2011. Re-scaling the Battjes-Janssen model for depth-induced wave breaking. *Proceedings of the 12<sup>th</sup> International Workshop on Wave Hindcasting and Forecasting*. WMO/JCOMM Technical Report No. 67. 13-6p.
- Schwab, W.C., Thieler, E.R., Allen, J.R., Foster, D.S., Swift, B.A., Denny, J.F., 2000. Influence of inner-continental shelf geologic framework on the evolution and behavior of the barrier-island system between Fire Island Inlet and Shinnecock Inlet, Long Island, New York. *Journal of Coastal Research*, 16, 408–422.
- Schwab, W.C., Baldwin, W.E., Hapke, C.J., Lentz, E.E., Gayes, P.T., Denny, J.F., List, J.H., Warner, J.C., 2013. Geologic evidence for onshore sediment transport from the inner continental shelf: Fire Island, N.Y. *Journal of Coastal Research*, 29, 526–544.
- Short, A.D. and Jackson, D.W.T., 2013. *Beach Morphodynamics*. In: Treatise on Geomorphology. (Eds: Shroder, John F.), Elsevier, Academic Press, Amsterdam, San Diego, 106-129.
- Smith, A., Mather, A., Guastella, L., Cooper, J.A.G., Ramsay, P.J. and Theron, A., 2010. Contrasting styles of swell-driven coastal erosion: examples from KwaZulu-Natal, South Africa. *Geological Magazine*, 147, 940-953.
- Soulsby, R., 1997. Dynamics of Marine Sands. Thomas Telford, London.

- Stive, M.J.F., Roelvink, D.J.A., and de Vriend, H.J., 1991. Large-scale coastal evolution concept. *Proceedings of the 22<sup>nd</sup> International Conference on Coastal Engineering*, New York. ASCE, 1962-1974.
- Stive, M.J.F., and de Vriend, H.J., 1995. Modeling shoreface profile evolution. *Marine Geology*, 126, 235-248.
- Stive, M. J. F., 2004. How important is global warming for coastal erosion? *Climate Change*, 64, 27–39.
- Thieler, E.R., Pilkey, O.H., Young, R.S., Bush, D.M., and Chai, F., 2000. The use of mathematical models to predict beach behavior for U.S. coastal engineering: A critical review. *Journal of Coastal Research*, 16, 48-70.
- Westley, K, Plets, R and Quinn, R.J., 2014. Holocene Paleo-Geographic Reconstructions of the Ramore Head Area, Northern Ireland, Using Geophysical and Geotechnical Data: Paleo-Landscape Mapping and Archaeological Implications. *Geoarchaeology* 29 (6), 411-430.
- Wright, L.D., and Short, A.D., 1984. Morphodynamic variability of surf zones and beaches: a synthesis. *Marine Geology*, 56, 93-118.
- Wright, L.D., Boon, J.D., Green, M.O., and List, J.H., 1986. Response of the mid shoreface of the southern mid-Atlantic Bight to a ‘northeaster’. *Geo-marine Letters*, 6, 153-160.
- Wright, L.D., Boon, J.D., Kim S.C., and List J.H., 1991. Modes of cross-shore sediment transport on the shoreface of the Middle Atlantic Bight. *Marine Geology*, **96**, 19–51.



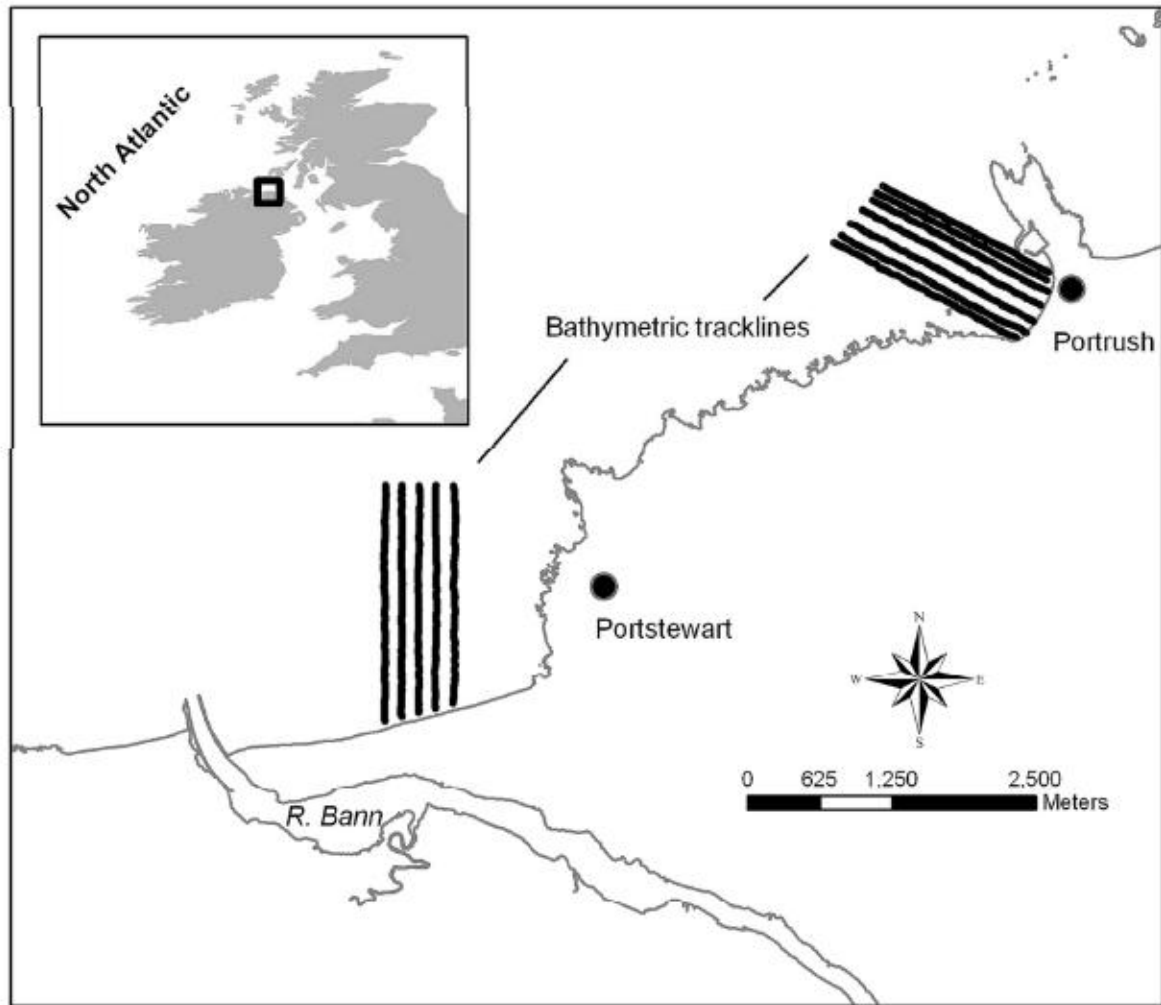


**Figure 1.** Study locations and bathymetric survey tracklines of Portstewart (lower left) and West Strand (upper right), Northern Ireland

Accepted



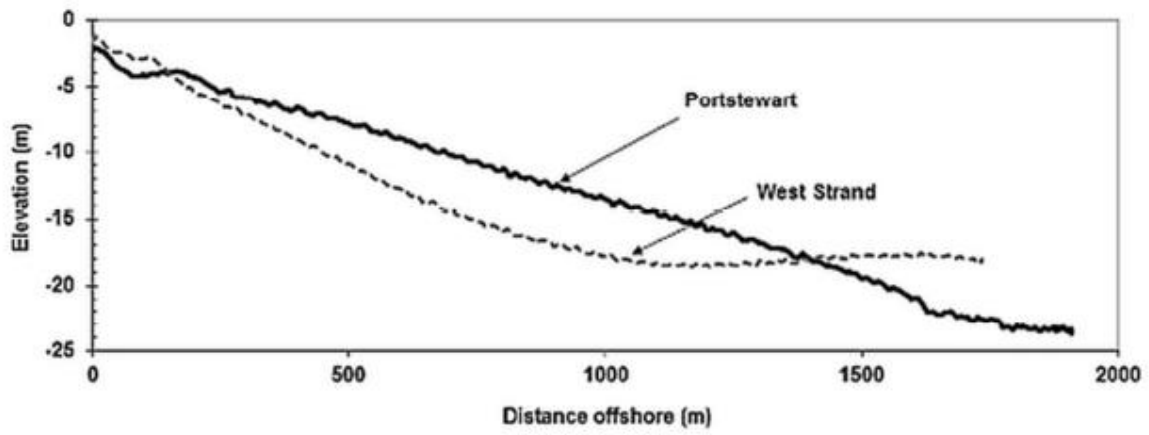


**Figure 2.** Typical shore-normal bathymetric profiles for Portstewart and West Strand

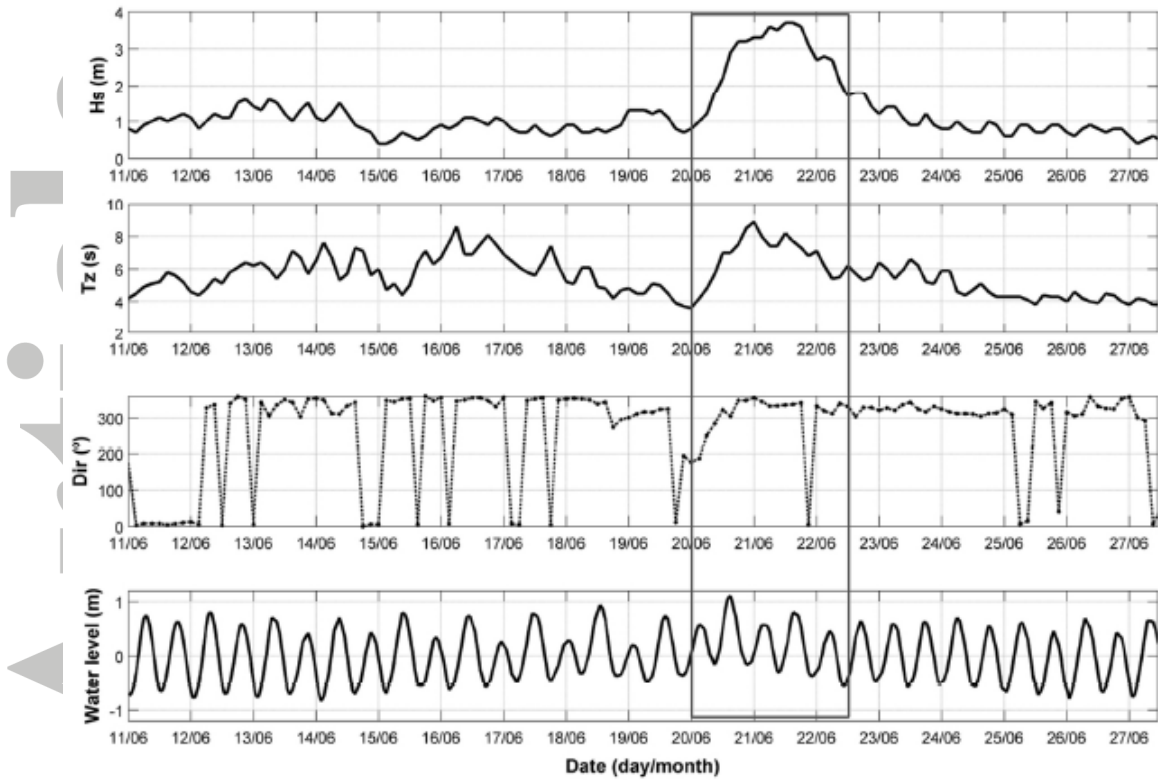


**Figure 3.** Significant wave height, wind speed, wind direction, and tide data covering period from pre- to post-storm surveys. The dashed rectangle (June 21st - June 23rd) corresponds to the storm.

Accepted

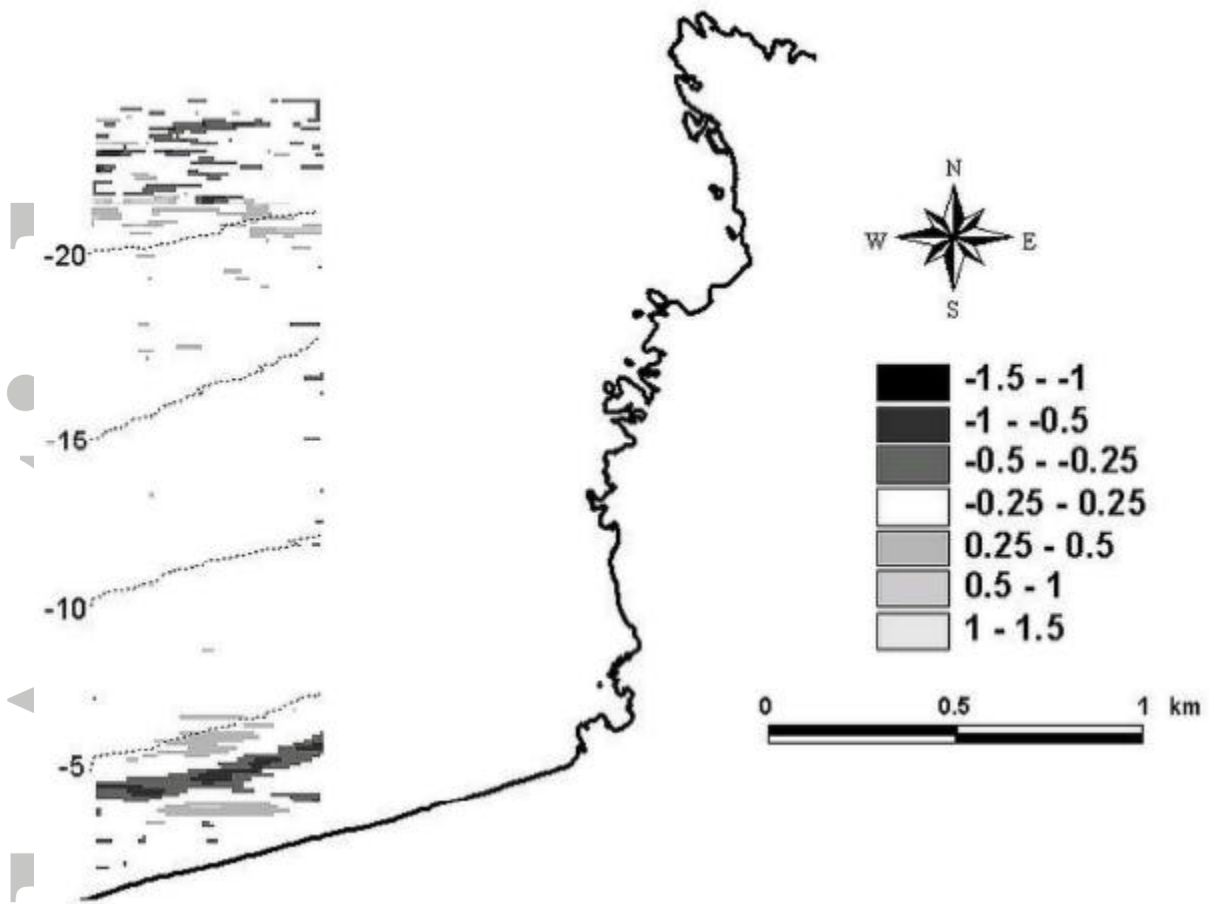


**Figure 4.** Storm-associated bathymetric difference map for Portstewart, generated by comparing June 11th and June 26th, 2006 survey data. The main seabed changes attributed to the storm are in the form nearshore bar changes.

Accepted

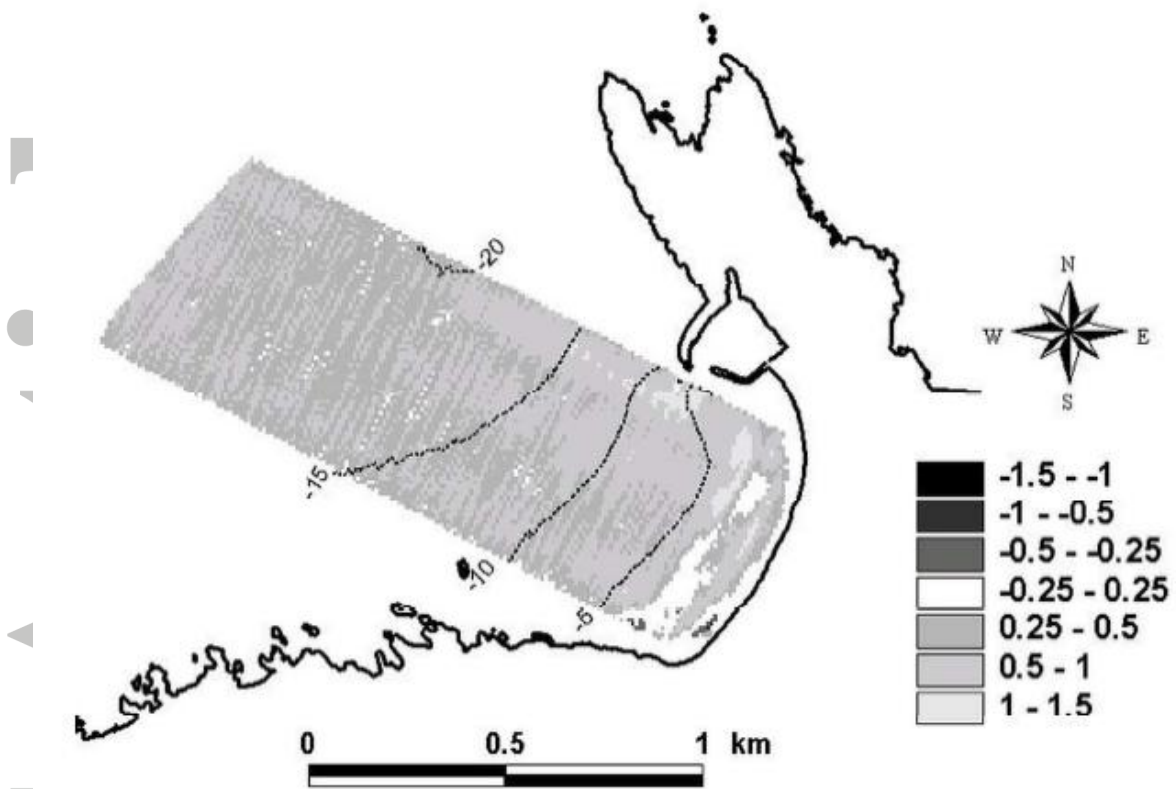


**Figure 5.** Storm-associated bathymetric difference map for West Strand, generated by comparing June 11th and June 26th, 2006 survey data. Note extensive shoreface-wide deposition attributed to the high-energy event, with minimal areas of erosion.

Accepted

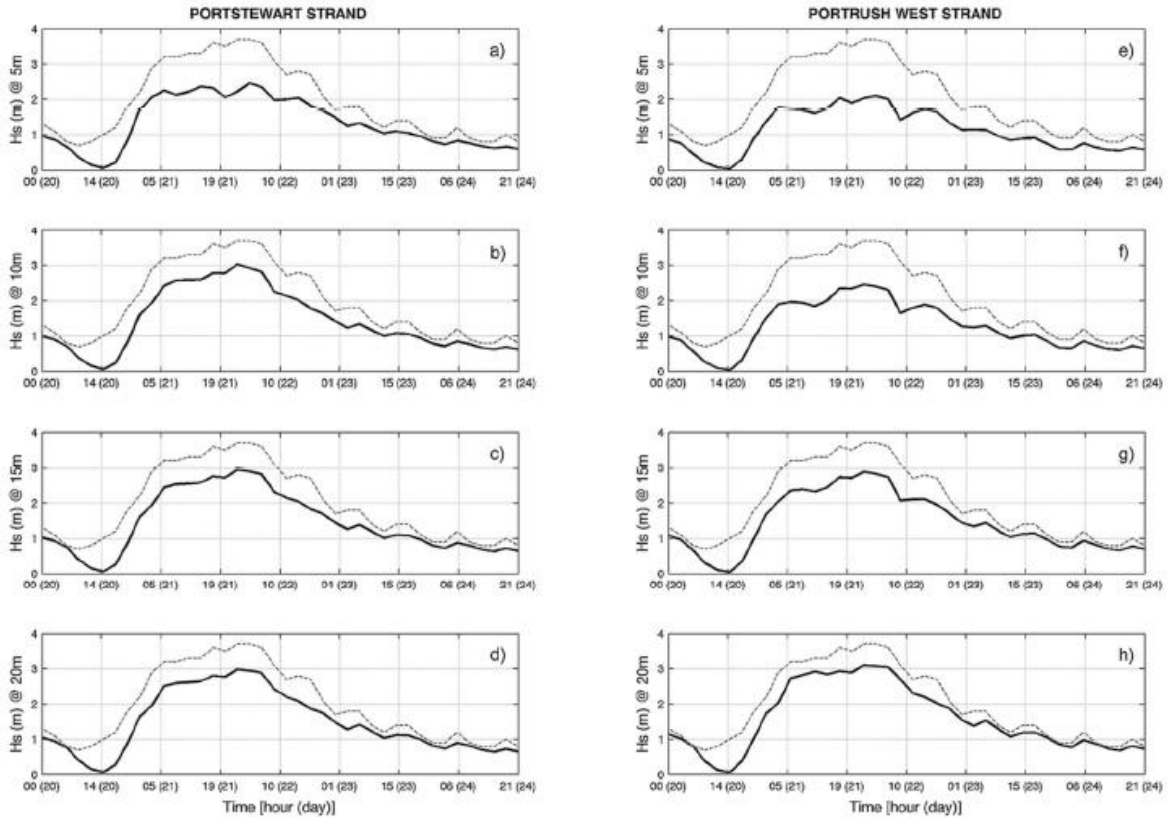


**Figure 6.** Time-series of nearshore wave height in the shoreface of Portstewart Strand (left panels) and Portrush West Strand (right panels), at 5 m, 10 m, 15 m and 20 m depths (offshore conditions displayed as dashed line).

Accepted

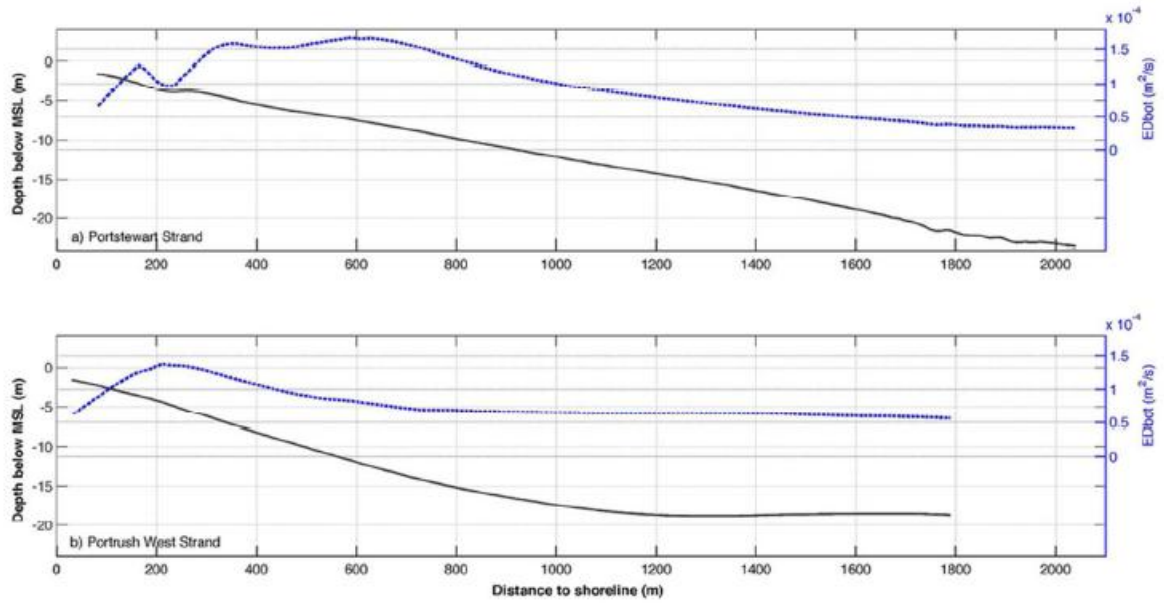


**Figure 7.** Energy dissipation due to bottom-friction (dashed blue line) along the nearshore profile (solid grey line) of Portstewart Strand (a) and Portrush West Strand (b). Modelled  $ED_{\text{bot}}$  values for the peak storm conditions at 00:00 of June 22<sup>nd</sup>.

Accepted

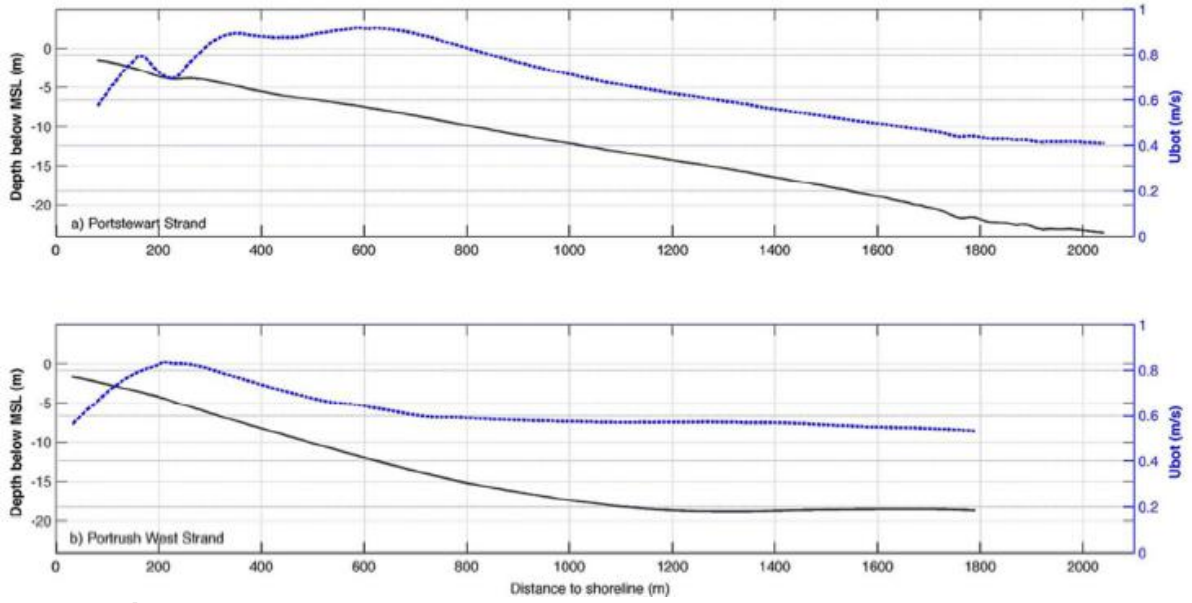


**Figure 8.** Near bottom maximum orbital velocities (dashed blue line) along the nearshore profile (solid grey line) of Portstewart Strand (a) and Portrush West Strand (b). Modelled  $U_{bot}$  values for the peak storm conditions at 00:00 of June 22<sup>nd</sup>.

Accepted



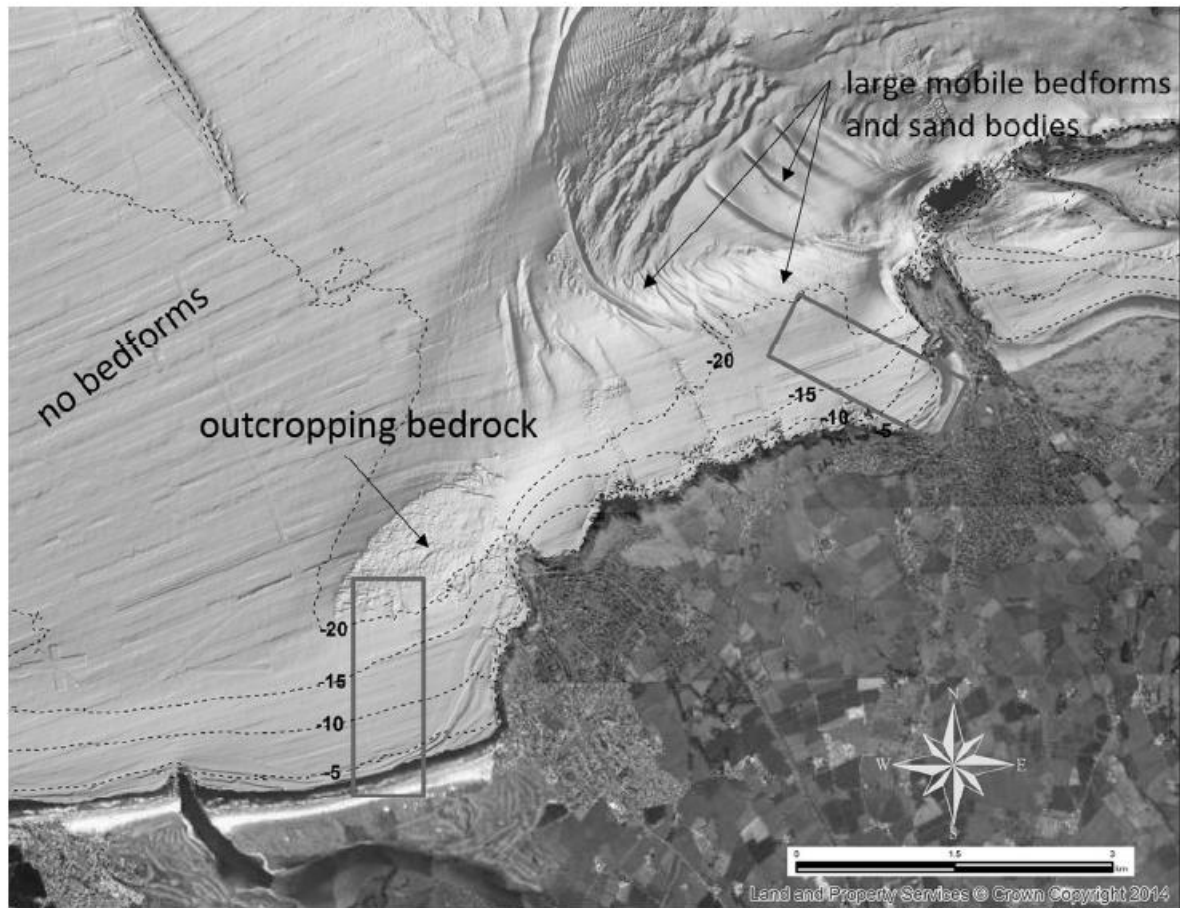


**Figure 9.** JIBS high-resolution multibeam bathymetry data collected in 2007. Note the presence of large sand bodies and mobile bedforms offshore of West Strand, seaward of 20 m depths, compared to the lack of bedforms and presence of outcropping bedrock at Portstewart.

Accepted